

COAGULATION EFFECTS

OF MICRO SIZED PARTICLES ON THE ATMOSPHERIC LIFETIME OF AIRBORNE ENGINEERED NANOPARTICLES

When measuring number concentrations of particles in different size modes, one will find different halftimes and / or transportation lengths. These differences are imposed by numerous mechanisms, such as dilution, deposition, nucleation, coagulation et cetera. This study points out the degree of significance of micro sized particles for coagulation of nanoparticles under various circumstances. Large particles have a higher coagulation rate per particle, but are present in lesser amounts; between these two we find a sensitive balance. An overview in extreme and regular particle concentrations is included, as well as a figure in which monodisperse coagulation effects are summarized. Particles with a diameter above 10 nm are generally not affected by any realistic amount of particulate matter with diameters above 2.5 μm . Particles with diameters above 10 μm do generally not contribute to coagulation loss of any particle, but atmospheric amounts of smaller particles do influence nanoparticles with diameters below 10 nm, such as quantum dots. Although coagulation due to micro sized particles is significant it never dominates over coagulation due to submicron particles. Monodisperse calculations appear to be of the same order of magnitude as continuous model calculations, and can function as minimum estimates.

Bachelor thesis
Gideon van den Brink
Universiteit Utrecht: Physics and Astronomy
June 2015

Prof. Dr. M. Dijkstra
Universiteit Utrecht : Debye Institute

Dr. J.S. Henzing
TNO Utrecht : Climate, Air and Sustainability



Universiteit Utrecht

TNO innovation
for life

CONTENTS

	Introduction	3
1.	Theory	4
1.1.	Coagulation rate	4
1.2.	Size dependence	5
2.	Method	6
2.1.	UHMA model	6
2.2.	The variable problem	6
2.3.	Input data acquisition	8
2.4.	Justification experiments	8
3.	Results	9
3.1.	Monodisperse coagulation study	9
3.2.	Justification experiments	11
4.	Conclusion	13
4.1.	Coagulation loss	13
4.2.	Monodispersity	13
4.3.	Recommendations	13
	References	14
Appendix A: Introduction to atmospheric particles		15
A.1.	Particle sizes	15
A.2.	Particle concentrations	15
A.3.	Particle size concentrations	16
A.4.	References	16
Appendix B: Tables and figures		17

Picture front page: a photograph of dust taken in Memphis (USA) by John Carey / fiftyfootshadows.net

INTRODUCTION

Nanotechnology has a very big technological and economic impact and even more potential, but little do we know about the risks of use. Where do (engineered) nanoparticles go when suspended into the atmosphere? Airborne particles in general are a form of air pollution that induces serious health effects; they are affected by numerous mechanisms: dilution, deposition, nucleation, coagulation et cetera. On top of that, airborne *nanoparticles* have interesting kinetic behavior, as they aren't big enough to move like macro sized particles (classical mechanics), but are also not small enough to move around like atoms or molecules (kinetic theory). In which form do we eventually find these nanoparticles, then? Do we breathe them, or eat them?

In this study I will focus on coagulation of nanoparticles (2-100nm). Coagulation occurs when particles collide and clump together.

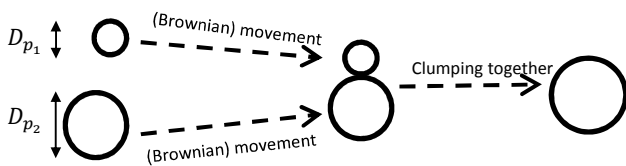


Figure 1 Schematic figure of a coagulation event of particles with diameters D_{p_1} and D_{p_2} .

TNO Utrecht has done previous research on coagulation effects in a project called NanoNext (2013). During the process several questions arose, which will have to be answered by the time new projects start.

In most research, only coagulation on particles with sizes of equal order is taken into account; This study focuses on the question whether and under what circumstances coagulation effects of bigger, micro sized, particles are important for the atmospheric lifetime of airborne engineered nanoparticles.

In this question, three sub questions are present: How do we express coagulation effects to get an overview for different particle sizes and concentrations; what are the particle population properties of different environments and finally, with coagulation in these environments found, what is considered significant?

In order to make calculations on coagulation, a multicomponent aerosol model developed at the University of Helsinki (Finland) is used. Circumstances of rural area, urban area, urban kerbside and near unpaved road are compared. To answer the question whether the found coagulation loss is significant, it is compared with the loss due to coagulation on nanoparticles (2-100 nm).

Note: I will directly get into the material, but have attached an introduction to atmospheric particles for the reader who's not familiar with this subject (Appendix A).

1. THEORY

1.1. COAGULATION RATE

Particles move under influence of Brownian, gravitational or other forces, and hence collide. Their collision rates depend on particle size, number concentration, and chemistry of the particles themselves and their many neighbors. Studying the coagulation effect on random particles, we thus first need to bring in all the different constituents that influence the collision rate¹ and next, multiply it with the probability of a coagulation event in case of a collision; a sticking probability.

As mentioned in the introduction, kinetic behavior of nanoparticles is not equal to that of particles in continuum (D_p above $1\mu\text{m}$), or in free molecular regime (D_p below 1 nm). In between these regimes we find a transition regime.

Continuum regime

To describe collisions between aerosol particles, we firstly assume that all particles are spherical. Although the atmosphere contains particles of many sizes that move with many different velocities, none of which is stationary, let's discuss the collision rate for an easier case: we want to find a collision rate between a set of moving particles and one stationary particle of the same radius R_p . What we need is a number of particles per unit of time whose center of mass is getting closer than $2R_p$ from the center of mass of our stationary particle. So we need the flux through the surface at $r = 2R_p$, which, in case of Brownian diffusion, can be found with Fick's first law (Fick, 1855):

$$\Phi = -D \left(\frac{\partial N}{\partial r} \right)_{r=2R_p} \quad (1)$$

in which D is the diffusion coefficient from the Stokes-Einstein equation (Einstein, 1905):

$$D = \frac{kT}{3\pi\mu D_p}$$

(with k the Boltzmann constant, T the temperature of the medium, μ the viscosity of air and $D_p = 2R_p$ the diameter of the particles) and $\partial N/\partial r$ the particle number concentration gradient which is constant $N_0/2R_p$ in steady state. N_0 is the particle number concentration at distance $r = \infty$ from our stationary particle; I will further leave out the subscript 0.

From equation 1 we can find the collision rate J_{col} by multiplying with the effective collision surface S_{eff} . Because our particles are moving in negative r direction, we can drop the minus-sign.

$$J_{col} = S_{eff} D \frac{N}{2R_p} \quad (3)$$

In the case of a set of moving particles and one stationary particle of the same radius R_p , we have an effective surface area of

$$S_{eff} = 4\pi(2R_p)^2, \quad (4)$$

Incorporating eq.3 in eq.4 gives us

$$J_{col_{stationary}} = 8\pi R_p D N. \quad (5)$$

Now, let's say that our stationary particle also undergoes Brownian diffusion and has another size than the rest of the particles. Let the subscript 1 indicate the smaller, and subscript 2 indicate the larger coagulation partner. $2R_p$ becomes $R_{p1} + R_{p2}$, the diffusion coefficient D becomes $D_{12} = D_1 + D_2$, N becomes N_2 and hence

$$J_{col_{moving}} = 4\pi(R_{p1} + R_{p2})(D_1 + D_2)N_2 \quad (6)$$

Adding a number of particles with diameter D_{p1} is now easy: if there are two particles, it is just $J_{col_{mov1}} + J_{col_{mov2}}$, which is the same as two times the original $J_{col_{mov1}}$. If there are N_1 particles, I thus add a factor of N_1 to eq.6:

$$J_{col_{continuum\ regime}} = 4\pi(R_{p1} + R_{p2})(D_1 + D_2)N_2 \quad (7)$$

This is the collision rate of particles in continuum regime, that is, with diameters above $1\mu\text{m}$.

¹ In this study, we don't bring in attractive forces (e.g. magnetism)

Free molecular and transition regimes

In this derivation, I have assumed Newtonian hard sphere boundary conditions in the calculation of $\partial N/\partial r$. When particles are getting smaller and smaller, however, a boundary layer has to be taken into account, with thickness of the mean free path λ , which is 65 nm in air. Also, the Stokes-Einstein equation (eq.2) must be corrected with a correction factor C_c^2 . Eventually, in the limit of very small particles, when particles are much smaller than λ , kinetic theory provides a collision rate J_{col} , (which I will not derive here):

$$J_{col} = \pi(R_{p_1} + R_{p_2})^2(\bar{c}_1^2 + \bar{c}_2^2)^{1/2}N_1N_2 \quad (8)$$

in which the mean thermal velocity $\bar{c}_i = (8kT/\pi m_i)^{1/2}$, with m_i the mass of the particles of species i . In between, we find the transition regime, and kinetic behavior is described with a match between the continuum and free molecular regimes. Fuchs suggested to solve this problem with a correction factor β^3 (Fuchs, 1964), such that

$$J_{col} = 2\pi(D_{p_2} + D_{p_1})(D_1C_{c_1} + D_2C_{c_2})\beta N_1N_2. \quad (9)$$

Note that this is an extensive expression, the limits of which are given in eq. 7 and 8. With eq. 9 we can obtain a collision rate J_{col} for all three regimes. Assuming the announced sticking probability to be $\alpha = 1^4$, we have found the monodisperse coagulation rate J_{12} of particles with diameters D_{p_1} and D_{p_2} :

$$J_{12} = 2\pi(D_{p_2} + D_{p_1})(D_1 + D_2)\beta N_1N_2 = K_{12}N_1N_2 \quad (10)$$

with K_{12} the so called coagulation coefficient.

² Known as the Cunningham correction factor. We do not need to elaborate on this factor for our case. It is a function of λ and D_p . Note however, that it approximates 1 for particles of diameter $> 0.5 \mu\text{m}$, and is bigger for smaller particles.

³ β is a dimensionless variable that varies from 0.014 for 1nm particles to 1 for 1 μm particles. The expression for β is rather extensive, but contains all the variables mentioned above, including the mean free path.

⁴ There is not much quantitative data on this sticking probability, but the low kinetic energy of aerosol particles makes bounce-off unlikely. If our assumption here is incorrect, however, and $\alpha < 1$, it will have a small impact on particles in the continuum regime. The effect is bigger for smaller particles.

1.2. SIZE DEPENDENCE

Roughly, we can conclude that, apart from temperature and medium, coagulation is dependent on particle sizes and their corresponding number concentrations. Coagulation dependence on number concentrations is linear, but the dependence on particle sizes is not: **figure 2** shows K_{12} as a function of particle size of the smaller particle D_{p_1} , for various values of particle size of the larger coagulation partner D_{p_2} as labeled. This is a key figure for understanding coagulation, and also the main inducement for this study. K_{12} is always minimal for particles of the same size (self-coagulation), as shown by the lowest thick line, and maximal for particles with maximal size difference.

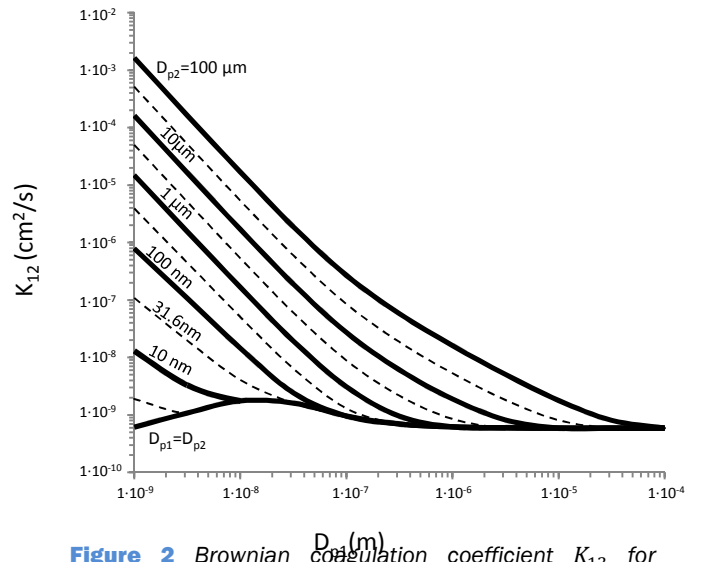


Figure 2 Brownian coagulation coefficient K_{12} for coagulation of particles diameters D_{p_1} and D_{p_2} . Find the smaller of the two particles and then locate the line corresponding to the larger particle. This figure is obtained by methods described later, but an equivalent can be found in Seinfeld and Pandis, 2006, pp.602. $T=283.15 \text{ K}$, $\mu=1.77 \cdot 10^{-4} \text{ g cm}^{-1}\text{s}^{-1}$

As mentioned in the introduction, most research on coagulation is conducted on homo-coagulation processes: collision of particles whose sizes are of the same order of magnitude. **Figure 2** gives reason to doubt that approach: K_{12} is maximal at maximal size difference, wouldn't J_{12} too? It is important to note, however, that number concentrations are higher for smaller particles than for bigger particles, leaving us with a sensitive balance between K_{12} , N_1 and N_2 , as qualitatively shown in **table 1**.

	Aitken	Accumulation	Coarse	Giant
N ₁	High	High	High	High
N ₂	High	Medium	Low	Lower
K ₁₂	Low	Medium	High	Higher
J ₁₂	High	High	?	?

Table 1 Qualitative insight in coagulation of Nucleation or Aitken mode particles on Aitken, accumulation, coarse or giant particles.

This raises the question how number concentrations and K_{12} relate to size, and which of the two has a steeper gradient. A priori, there is no reason to disqualify coagulation between different size modes. On the other hand, micro sized particles have limitations on their number concentrations, so there is no reason to a priori consider it a major effect.

2. METHOD

2.1. THE UHMA MODEL

In order to execute calculations on atmospheric coagulation processes, I have been working with a multicomponent aerosol model developed at the University of Helsinki (Finland). This model, abbreviated as UHMA-model (Korhonen et al., 2004), executes calculations by methods described in the theory section. It is written in Fortran90.

Input

To initialize the model, give it a file (named `distr.dat`) which contains a minimum and maximum radius in order to calculate the size bins; on the next rows, it contains a number concentration ($\#/m^3$), a mean radius (m) and a geometric standard deviation for each different lognormal size mode one wants to add. More advanced inputs are possible for condensable aerosols, but we can neglect those options for our cause. One other initializing file is used (named `ambient.dat`), in which the desirable time steps and duration of the model experiment are given, as well as some more detailed settings we need not worry about, such as temperature.

Throughput

First, the UHMA model reads the input-file, and creates a number of bins (default 25) of radii that are

logarithmically equidistant between the given minimum and maximum radius. Next, neat lognormal distributions of number concentrations as a function of particle radius are created for each mode given. The number concentrations are now given in terms of:

$$\frac{dN}{d \log D_p} = \frac{N_{total}}{\sqrt{2\pi} \log \sigma_g} \exp\left(-\frac{\left(\log \frac{R_{bin}}{R_{mode}}\right)^2}{2 \log \sigma_g}\right) \quad (11)$$

In which N_{total} would be the sum of the given number concentrations of the modes, the total number concentration ($\#/m^3$). This is our data at $t = 0$. In this subroutine, the calculates the coagulation coefficients and rates between all combinations of size bins according to the aforementioned formulae and a matching subroutine between the different regimes (continuum and gaseous). Integrating these rates over a time step gives our loss of particles in each bin, which will be subtracted of the number of particles of that particular bin. Next, the new radius of the joint particle is computed, and the particle will be placed in the appropriate size bin. Note that nanoparticles will grow due to coagulation, but coarse particles do not (significantly). Still, a collision always leads to the disappearance of one particle. Total volume is constant.

Output

The UHMA-model is written neatly and organized, so that any variable mentioned above is easily found in the code. Initially, it wrote radii and number concentrations at time t in seconds to separate files. The model is adapted in such a way that it also served a tool to compute coagulation coefficients K_{12} .

2.2. THE VARIABLE PROBLEM

Size and number concentrations are the main variables for coagulation⁵. Since two particles are needed for one collision, we have a coagulation rate dependent on four variables: $J_{12}(D_{p_1}, D_{p_2}, N_1, N_2)$. To

⁵ This study does not elaborate on temperature and medium, which are equal for all particles in a certain environment. Also, atmospheric values do not differ as widely as particle size and number concentration do.

gain insight in coagulation processes in general is therefore a multivariable problem. However, as I am interested in the influence of the bigger particle mode on the atmospheric lifetime⁶ of the smaller one, I do not want to know the *number* of particles lost per time J_{12} , but rather the *fractional loss* of my smaller particles

$$\frac{J_{12}}{N_1} = K_{12} N_2 (D_{p_1}, D_{p_2}, N_2) \quad (12)$$

Since I already know what $K_{12}(D_{p_1}, D_{p_2})$ looks like (**figure 2**), I only have to multiply it by N of the coagulation partner of interest: I now have lost one degree of freedom.

Although J_{12}/N_1 only provides knowledge on coagulation due to N particles of exactly size 2 on particles with exactly diameter 1, and not on continuous distributions, this is already insightful: per smaller particle I only have two degrees of freedom. Per set of partners, I only have 1 degree of freedom. I will provide an example to clarify how this information can be used.

Imagine I want to know the coagulation loss of 10 nm particles due to a number (yet to be determined) of 1 μm - particles. **Figure 2** gives me that $K_{12} = 1,67 \cdot 10^{-7} \text{ cm}^3/\text{s} = 6,01 \cdot 10^{-10} \text{ m}^3/\text{h}$. Multiplied with N_2 this gives the fractional loss of particles with diameter 10 nm due to coagulation on particles with diameter 1 μm , as shown in **figure 3**.

I know from **figure 2** that K_{12} will have higher values for larger D_{p_2} , and lower values for smaller D_{p_2} . **Figure 4** shows how some values of $J_{12}/N_1(N_2)$ compare. Indeed, lines that indicate coagulation with a larger partner are situated higher in the plot; still, they do not necessarily indicate a higher coagulation loss, because particle modes each carry another value of N_2 . I thus need information on the characteristic concentrations of particles with these diameters $N_2(D_p)$ in different environments.

⁶ I have not introduced this term. Although it is a very important notion, I will not mention this exact word again. It means: time after which my initial concentration is decreased to a portion of $1/e$ the initial concentration.

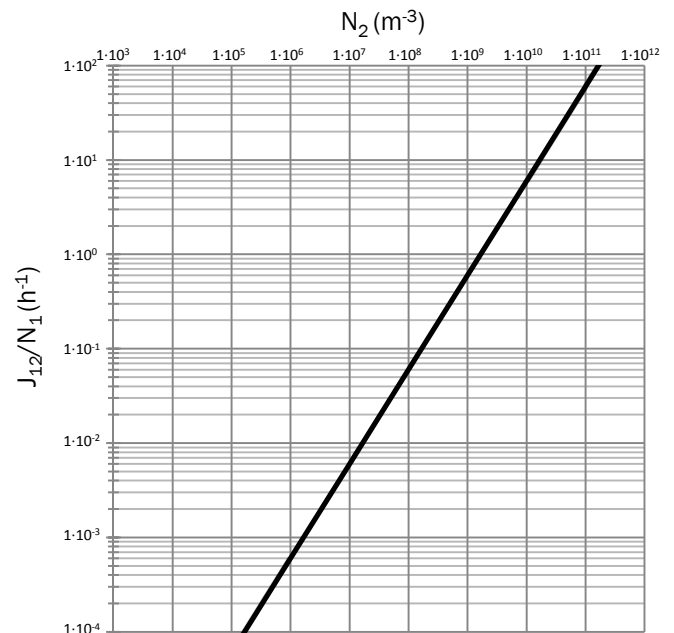


Figure 3 Fractional loss of particles with diameter 10 nm due to coagulation with a concentration N_2 of particles with a diameter 1 μm .

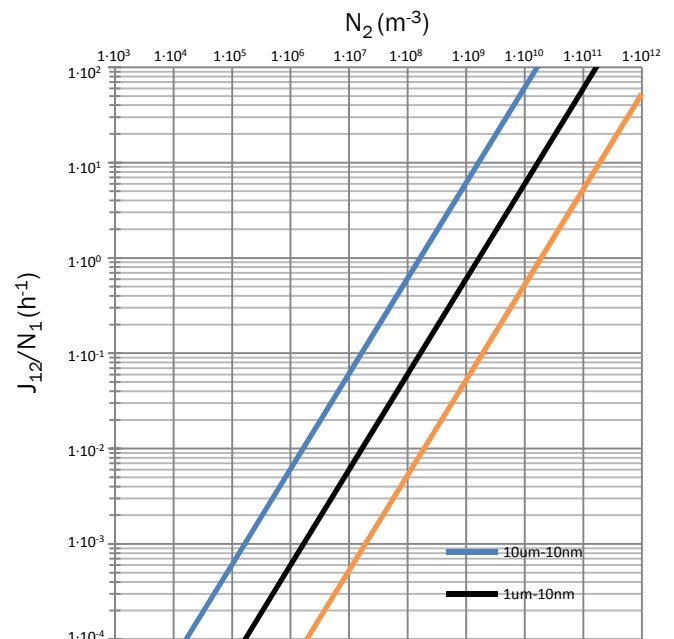


Figure 4 Fractional loss of particles with diameter 10 nm due to coagulation with a concentration N_2 of particles with diameters 0.1, 1 and 10 μm . Lines are parallel due to their linearity in N_2 . Lines are not equidistant: their heights are given by K_{12} , which is non-linear.

Further, although each line only has 1 degree of freedom, I should still draw # size bins lines per D_{p_1} , for all different D_{p_1} 's. To simplify this, I only take a few particle sizes into account, which leads to a problem of only a few variables: $J_{12}(D_{p_1-N}, N_{1-N})$. For these sizes, we can construct a figure like **figure 4**, containing a number of lines to show the fractional coagulation loss due to large particles, to which lines that show homo-coagulation can be added.

Note that with this simplification, a lot less input information is used or required. In order to make this simplification, I have made assumptions I need to justify. This study thus consist of two parts: first, answering the research questions with the methods described above. Next, a number of experiments is set up to justify working monodisperse.

2.3. INPUT DATA AQUISION

Particle modes

The main aim of this study is to gain knowledge on coagulation loss of nanoparticles, ranging from 2-100 nm, due to collision with micro-sized particles. The following experiments are executed with particle diameters 2.37 nm, 10.0 nm, 31.6 nm and 100 nm as insightful landmarks of nano-scale particles. Since micro sized particles measured are mass-based, the following diameters are chosen to represent PM2.5, PM10 and TSP modes: 1.54 μm , 3.16 μm and 31.6 μm respectively. In order to translate between mass and number densities, a density of approximately 1,2 g/cm^3 is assumed, and all particles are assumed spherical.

Particulate matter characteristics

Table 2 shows extreme and regular mass concentrations of particulate matter. Measurements vary widely per study, so read the values as indicative values. Indoor/outdoor ratios of particulate matter vary between 0.5 and 2, sometimes higher values are reported (Morawska and Salthammer, 2003; Liu et al., 2004). The World Health Organization (WHO, 2006) uses 10 $\mu\text{g}/\text{m}^3$ annual mean, 25 $\mu\text{g}/\text{m}^3$ 24-hour mean as guideline values for PM2.5 and 20 $\mu\text{g}/\text{m}^3$ annual mean, 50 $\mu\text{g}/\text{m}^3$ 24-hour mean as guideline values for PM10.

	Unpaved road ⁷	Urban kerbside ⁸	Urban backgr. ^{9,9}	Rural backgr. ¹⁰
TSP _{mean}	1560	122	96/40	24
TSP _{max}	3600	377	466/194	79
TSP _{min}	760	42	15/6	10
PM10 _{mean}	1130	76	23/28	21
PM10 _{max}	2420	214	95/120	53
PM10 _{min}	640	37	1/3	4
PM2.5 _{mean}	570	57	8/19	15
PM2.5 _{max}	1610	122	65/81	48
PM2.5 _{min}	240	28	0.5/2	3

Table 2 Rough indication of mass concentrations in different environments. Concentrations are given in $\mu\text{g}/\text{m}^3$.

Nanoparticles characteristics

Table 3 shows extreme and regular number concentrations. N.B. These are important as a significance check, but not necessary for studying coagulation loss due to (super)coarse particles.

	Unpaved road	Urban kerbside ¹¹	Urban backgr. ¹⁰	Rural backgr. ¹²
N _{mean}	unknown	$3 \cdot 10^{10}$	$5 \cdot 10^9$	$4 \cdot 10^9$
N _{max}	unknown	$1 \cdot 10^{11}$	$3 \cdot 10^{10}$	$1 \cdot 10^{10}$
N _{min}	unknown	$6 \cdot 10^9$	$5 \cdot 10^8$	$1 \cdot 10^8$

Table 3 Rough indication of number concentrations in different environments. Concentrations are given in m^{-3} .

2.4. JUSTIFICATION EXPERIMENTS

It is not evident that we are allowed to work with figures like **figure 4** made up from the input data I described: it says that, for example, the total number of particles with a diameter below 10 μm is translated to the same number of particles with a diameter of exactly 3.16 μm . An assumption that would be more agreeable, is that these particles were to be lognormal distributed around a mean diameter of 3.16 μm (the lognormal middle between 1 and 10 μm) with a geometric standard deviation σ_g that we allow to vary.

⁷ Chang, 2006

⁸ Chan and Kwok, 2001

⁹ Bayraktar et al., 2010

¹⁰ Gomiscka, 2004

¹¹ Wang et al., 2010

¹² Asmi et al., 2011

In order to examine the difference between the two, the UHMA-model can be used: I can compare the coagulation loss inside a nanobin due to a monodisperse and several wider modes of coarse material. The nanobin carries a low enough number concentration, so that its self-coagulation rate is insignificant compared to the coagulation-rate from the larger particle bin. I have chosen to work with 0.01cm^{-3} . I have repeated this for $1.54\ \mu\text{m}$, $3.16\ \mu\text{m}$ and 31.6 . In order to stay in a linear regime, I have adapted the concentration in the (super)coarse bin so that the coagulation loss is of order 1%/h or lower. This is experiment 1.

Also, one might not be interested in the loss of nanoparticles with an exact size, but rather in a modal collection with that size as mean diameter. In order to examine the difference between these, we compare the fractional coagulation loss in the modal mean bin and in the sum over all nanobins of interest due to a monodisperse dust mode for several values of σ_g . This is repeated at 2.37, 10, 31.6 and 100 nm. This is experiment 2.

These experiments wouldn't be complete without also comparing monodisperse output with the output from two wider modes; this will be experiment 3.

Table 6 in section 3.2. shows the model input data and results for these experiments simultaneously.

3. RESULTS

3.1. MONODISPERSE COAGULATION STUDY

With the UHMA-model, the following values of K_{12} are obtained:

	2.37 nm	10 nm	31.6 nm	100nm
1.54 μm	$4.34\cdot 10^{-6}$	$2.60\cdot 10^{-7}$	$2.97\cdot 10^{-8}$	$4.55\cdot 10^{-9}$
3.16 μm	$9.10\cdot 10^{-6}$	$5.37\cdot 10^{-7}$	$6.05\cdot 10^{-8}$	$8.91\cdot 10^{-9}$
31.6 μm	$9.26\cdot 10^{-5}$	$5.39\cdot 10^{-6}$	$6.00\cdot 10^{-7}$	$8.54\cdot 10^{-8}$

Table 4 Coagulation coefficients K_{12} (cm^3/s) for nano-micro coagulation.

	2.37 nm	10 nm	31.6 nm	100nm
100 nm	$1.79\cdot 10^{-7}$	$1.46\cdot 10^{-8}$	$2.43\cdot 10^{-9}$	$9.58\cdot 10^{-10}$
31.6 nm	$3.02\cdot 10^{-8}$	$4.08\cdot 10^{-9}$	$1.61\cdot 10^{-9}$	
10 nm	$4.48\cdot 10^{-9}$	$1.76\cdot 10^{-9}$		
2.37 nm	$9.41\cdot 10^{-10}$			

Table 5 Coagulation coefficients K_{12} (cm^3/s) for nano-nano coagulation.

With these coagulation coefficients, and information from table 3 and 4, **figure 5** is plotted, in which answers to the research questions posed in the introduction are summarized. The lines are cut off at unrealistic concentrations in ambient air. As mentioned, indoor concentrations are of the same order of magnitude.

When studying **figure 5**, note the following: based on the rural background minimum from **table 3** and a self-coagulation coefficient of $6.34\cdot 10^{-12}\ \text{h}^{-1}$ nanomode-coagulation loss is always above $6.34\cdot 10^{-4}\ \text{h}^{-1}$. Based on rural and urban mean values from **table 3** and the aforementioned self-coagulation coefficient, regular nanomode-coagulation is above $3.17\cdot 10^{-2}\ \text{h}^{-1}$. These are ambient absolute and regular minima, based on pure self-coagulation: coagulation with particles of the (exact) same size. As particles are distributed over a certain range of size, there is always a certain size difference and nanomode-coagulation coefficients will always be bigger than coefficients for monodisperse self-coagulation. Aitken mode particles are distributed around a value somewhere around 30-50 nm (Asmi et al); $D_p(N_{\text{max}})$ is also considered to be in this region.

Also note that for any size of (super)coarse material, a value for any nanoparticle can be interpolated. If, for example, interested in nanoparticles of 20 nm, one can estimate a value between the second and third lines vertically. Note the logarithmic scales. Calculations should be done with the model, but this method provides a quick tool for estimating the significance of different coagulation partners.

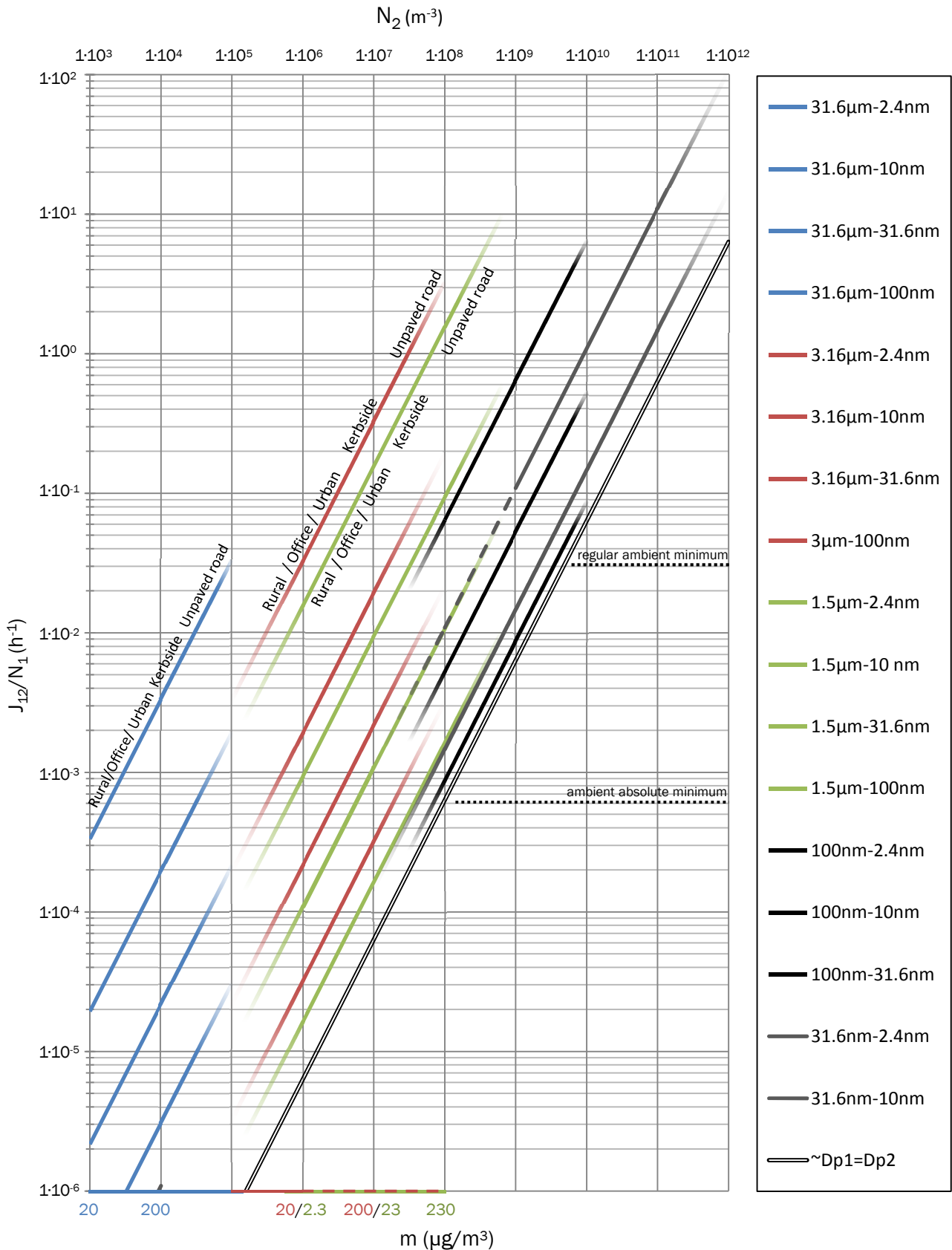


Figure 5 Fractional loss of smaller particles per hour for coagulation of particles diameters D_{p1} and D_{p2} , with growing number of bigger particles $N_2 \text{ (m}^{-3}\text{)}$. Each line represents a combination of a bigger and a smaller particle diameter. Find the line of interest, on the horizontal axis find the total number (upper axis), or the total mass (lower axis) of the bigger particles. Blue indicates particles with (mean) $D_{p2}=31.6 \mu\text{m}$, a good estimate for TSP; red indicates particles with (mean) $D_{p2}=3.16 \mu\text{m}$, a good estimate for PM10; green indicated particles with $D_{p2}=1.54 \mu\text{m}$, a good estimate for PM2.5. One grey line (31.6 nm-2.37 nm) is dashed because of overlap with a green line (1.54 µm-31.6 nm). Lines are labeled at approximate values per environment. Compare [table 2](#). To be correct: N_2 is to be defined as $\int (dN_2/d\text{Log}D_{p,2})d\text{Log}D_p$. $T=283.15 \text{ K}$, $\mu=1.77 \cdot 10^{-4} \text{ g cm}^{-1}\text{s}^{-1}$

Of the blue lines, indicating coagulation on supercoarse particles, only the upper two ($D_{p_1} = 2.37$ and 10 nm) reach to a height of the same order of the ambient absolute minimum. It is unlikely that there is a maximum of supercoarse material and a minimum of nanoparticles, and it is therefore unlikely that supercoarse material has a major coagulation effect on nanoparticles of 10 nm and bigger. Comparing the upper blue line with the upper red, green, black and grey lines however, we see that the latter each indicate a coagulation loss a 10-100 times higher. Supercoarse material is thus also not considered to have a major effect on particles of size $D_{p_1} = 2.37$. and therefore on any nanoparticle. Although there are situations possible in which coagulation on supercoarse particles is significant, this is not the case for normal ambient conditions.

Of the red lines, indicating coagulation on coarse particles, all four reach to the level of the ambient absolute minimum, however, only the upper two reach the minimal level of regular coagulation. As for the second line (nanoparticles of size 10 nm), the loss due to coarse material is in most environments, around 10 times smaller than loss due to homo-coagulation. Still, it should not a priori be disregarded when interested in nucleation mode particles. This influence of coarse material wanes above 10 nm.

Of the green lines, indicating coagulation on particles with diameter $2.5 \mu\text{m} > D_{p_2} > 1 \mu\text{m}$, again all four reach to the level of the ambient absolute minimum. The upper three now reach to the regular minimum level of homo-coagulation, therefore these particles are not to be ignored when interested in coagulation loss of (small) nanoparticles.

Note that, by definition, PM2.5 is also part of PM10 mass concentrations. Therefore, they should not be compared as separate modes. It is by definition impossible that PM10 coagulation loss is smaller than PM2.5 loss, although the plotted lines indicate otherwise. From this we can conclude that in extreme conditions, a mean diameter of $3.16 \mu\text{m}$ is no longer an accurate assumption. Still, in all circumstances, a major part of coarse material coagulation loss is due to particles with diameter $D_{p_2} < 2.5 \mu\text{m}$. K_{12} does not grow as fast with D_p as volume does.

Concluding, particles with a diameter above 10 nm are generally not affected by any realistic amount of particulate matter with diameters above $2.5 \mu\text{m}$. Particles with diameters above $10 \mu\text{m}$ do generally not contribute to coagulation loss of any particle, but atmospheric amounts of coarse material do influence nanoparticles with diameters below 10 nm, such as quantum dots. Coagulation due to atmospheric amounts of micro sized particles is, though, never considered bigger than coagulation due to submicron particles.

3.2. JUSTIFICATION EXPERIMENTS

In [table 6](#), the input and results are shown for experiments 1,2 and 3 as described in the method section.

In general, coagulation effects are bigger with a wider particle mode: results in the previous section thus indicate lower estimates.

Experiment 1 reveals that this effect of a wider coarse particle distribution is increasing with mean particle size. Coagulation loss from wider modes is still of the same order as loss calculated from monodisperse modes. Maximal difference is +50%.

Experiment 2 reveals that the effect of a wider nanoparticle distribution is also increasing with mean particle size, and is still of the same order as loss calculated from monodisperse modes, but is bigger. Maximal difference is +110%.

Experiment 3 measures how these effects add up. Two wider modes cause an even larger loss than the sum of the two effect. Maximal difference in this experiment is +214%, but is expected to be larger if computed for a nanomode of 100 nm. Also for two wide modes, coagulation loss is of same order as obtained through monodisperse calculations.

Coagulation of nucleation mode particles on (small) coarse particles shows minimal difference between monodisperse and continuous calculations: +163% or less.

Exp.1		Nanomode			Micromode			Result	
Exp.1		μ	N	σ_g	μ	N	σ_g	Loss (%/h)	Cont/Mono
1.1	1.1.1	10 nm	0.01 cm ⁻³	1	1.54 μ m	10 cm ⁻³	1	0.93	1
	1.1.2						1.5	1.01	1.09
	1.1.3						2	1.19	1.28
1.2	1.2.1	10 nm	0.01 cm ⁻³	1	3.16 μ m	10 cm ⁻³	1	1.9	1
	1.2.2						1.5	2.1	1.11
	1.2.3						2	2.5	1.32
1.3	1.3.1	10 nm	0.01 cm ⁻³	1	31.6 μ m	1 cm ⁻³	1	1.6	1
	1.3.2						1.5	2.1	1.31
	1.3.3						2	2.4	1.50
Exp.2		μ	N	σ_g	μ	N	σ_g	Loss (%/h)	Cont/Mono
2.1	2.1.1	2.37 nm	0.01 cm ⁻³	1	3.16 μ m	1 cm ⁻³	1	3.2	1
	2.1.2			1.5				4.1	1.28
	2.1.3			2				4.5	1.41
2.2	2.2.1	10 nm	0.01 cm ⁻³	1	3.16 μ m	10 cm ⁻³	1	1.9	1
	2.2.2			1.5				2.9	1.53
	2.2.3			2				4.9	2.58
2.3	2.3.1	31.6 nm	0.01 cm ⁻³	1	3.16 μ m	10 cm ⁻³	1	0.22	1
	2.3.2			1.5				0.34	1.55
	2.3.3			2				0.62	2.82
2.4	2.4.1	100 nm	0.01 cm ⁻³	1	3.16 μ m	10 cm ⁻³	1	0.031	1
	2.4.2			1.5				0.041	1.32
	2.4.3			2				0.065	2.10
Exp.3		μ	N	σ_g	μ	N	σ_g	Loss (%/h)	Cont/Mono
3.1	3.1.1	2.37 nm	0.01 cm ⁻³	1	3.16 μ m	1 cm ⁻³	1	3.2	1
	3.1.2			1.5			5.5	1.72	
	3.1.3			2			5.9	1.84	
3.1	3.2.1	10 nm	0.01 cm ⁻³	1	3.16 μ m	10 cm ⁻³	1	1.9	1
	3.2.2			1.5			3.4	1.80	
	3.2.3			2			5.0	2.63	
3.3	3.3.1	31.6 nm	0.01 cm ⁻³	1	3.16 μ m	10 cm ⁻³	1	0.22	1
	3.3.2			1.5			0.38	1.73	
	3.3.3			2			0.69	3.14	

Table 6 Coagulation loss of particles in the nanomode after 1 hour. The column ‘Cont/mono’ indicates the fraction of continuously calculated loss over monodispersely calculated loss. Input as described for experiments 1,2 and 3 in the method section. A σ_g of 1 indicates a monodisperse result; however, The UHMA-model does not allow a σ_g of 1. Monodisperse coagulation losses are either obtained through multiplication of K_{12} with N_2 (method used in figure 5), or through a model run with a σ_g of 1.0001: a value small enough to ensure all particles will be placed in the same size bin. These methods lead to the same results.

4. CONCLUSIONS

This study provides insight in coagulation loss due to (super)coarse material. The coagulation coefficient between large particles and nanoparticles is up to a million times larger than the coagulation coefficient between two nanoparticle concentrations. On the other hand, number concentrations of large particles can also be of order million times lower than nanoparticle concentrations. Between coagulation coefficient and number concentrations there is a sensitive balance we cannot conclude on without taking note of environment properties. This study therefore includes an overview in extreme and regular particle concentrations, on the basis of which the significance of coagulation loss terms are determined in a general way.

4.1. COAGULATION LOSS

Under normal circumstances, monodisperse research indicates that particles with a diameter bigger than 10 μm do not significantly contribute to the coagulation loss of nanoparticles. A significant amount of nucleation mode particles may, depending on environment, coagulate with coarse material. Coagulation loss due to these micro-sized particles reaches values comparable to (although smaller than) loss due to homo-coagulation. It is most significant in cases that the ambient nanoparticles have low number concentration and mean diameter, and there is a maximum amount of coarse mode material.

Given a certain mass concentration, coagulation of nanoparticles is maximized if the mean diameter of the coarse material is low: K_{12} does not grow as fast with D_p as volume does. Note that this only holds given a certain mass concentration: K_{12} does not necessarily have a steeper gradient than N does.

Apart from these general conclusions, **figure 5** can be used to determine the coagulation loss, given the particle size distribution in any environment. When dealing with intermediate particle sizes, an estimate of coagulation loss can be obtained by eye.

4.2. MONODISPERSITY

The experiments in this study indicate that the modal values are always higher than the values obtained with monodisperse experiments. Values in figure 5 therefore represent lower estimates: actual values are always higher.

Although actual values are higher, they are still of the same order. Differences are smallest (below +163%) for modes that are of most interest (nucleation mode and small coarse material).

These findings ensure that the aforementioned conclusions are correct and estimates of coagulation loss obtained by monodisperse calculation are of the right order of magnitude, even with wide particle size distributions (a σ_g of 2 is large in ambient air (Asmi et al., 2011)).

4.3. RECOMMENDATIONS

Significance of coagulation effects can also be compared with nucleation, dilution and deposition effects to gain more insight in its influence on lifetime.

This study also encourages to do more research on the influence of the width of particle modes, i.e. differences between monodisperse and modal calculations. More accurate conclusions can be drawn if more knowledge in this subject is present.

In this study assumptions are made on number concentration distributions of coarse material which are possibly unaccurate. This study mainly lacks information on the number concentration (gradient) (in the smaller part) of coarse material.

REFERENCES

- Asmi, A. et al. (2011) 'Number size distributions and seasonality of submicron particles in Europe 2008–2009', *Atmospheric Chemistry and Physics*, Vol. 11, pp. 5505–5538.
- Bayraktar, H. et al. (2010) 'Average mass concentrations of TSP, PM10 and PM2.5 in Erzurum urban atmosphere, Turkey', *Stochastic Environmental Research and Risk Assessment*, Vol. 24, Issue 1, pp. 57–65.
- Chan, L.Y. and Kwok, W.S. (2001) 'Roadside suspended particulates at heavily tracked urban sites of Hong Kong: Seasonal variation and dependence on meteorological conditions', *Atmospheric Environment*, Vol. 35, pp. 3177–3182.
- Chang, C.T. (2006), 'Characteristics and Emission Factors of Fugitive Dust at Gravel Processing Sites', *Aerosol and Air Quality Research*, Vol. 6, No. 1, pp. 15–29.
- Einstein, A. (1905), 'On the movement of small particles suspended in stationary liquids required by the molecular-kinetic theory of heat', *Annalen der Physik*, Vol. 17, pp. 549–560.
- Fick, A. (1855), 'Ueber Diffusion', *Poggendorfs Annalen der Physik und Chemie*, Vol. 170, No. 4, Series 94, pp. 59–86.
- Fuchs, N.A. (1964) *The Mechanics of Aerosols*, translated by R. E. Daisley and Marina Fuchs - edited by C. N. Davies, London: Pergamon Press
- Gomisceka, B. et al. (2004) 'Spatial and temporal variations of PM1, PM2.5, PM10 and particle number concentration during the AUPHEP–project', *Atmospheric Environment*, Vol. 38, pp. 3917–3934.
- Korhonen, H. et al., (2004) 'Multicomponent aerosol dynamics model UHMA: model development and validation' *Atmospheric Chemistry and Physics*, Vol. 4, pp 757–771.
- Leaderer, B.P. et al. (1999) 'Indoor, Outdoor, and Regional Summer and Winter Concentrations of PM₁₀, PM_{2.5}, S₄₋₂, H⁺, NH₄⁺, NO₃⁻, NH₃, and Nitrous Acid in Homes with and without Kerosene Space Heaters', *Environmental Health Perspectives*, Vol.107, No.3, pp. 223–231.
- Liu, Y. et al. (2004), 'Wintertime indoor air levels of PM₁₀, PM_{2.5} and PM₁ at public places and their contributions to TSP', *Environment International*, Vol. 30, No. 2, pp. 189–197.
- Morawska, L. and Salthammer, T. (2003), *Indoor Environment: Airborne Particles and Settled Dust*, Weinheim: Wiley-VCH
- Philipse, A.P. (2011), *Notes on Brownian Motion*, Utrecht University: Debye Institute. Available from : http://userpages.umbc.edu/~dfrey1/ench630/philipse_notes_on_brownian_motion.pdf (17-6-2015)
- Rajh, T. et al. (1993) 'Synthesis and characterization of surface-modified colloidal cadmium telluride quantum dots', *Journal of Physical Chemistry*, 97 (46), pp 11999–12003.
- Seinfeld, J.H. and Pandis, S.N. (2006) *Atmospheric chemistry and physics*, 2nd edition, Hoboken: John Wiley and Sons, Inc.
- Wang, F. et al. (2010) 'Particle number, particle mass and NO_x emission factors at a highway and an urban street in Copenhagen', *Atmospheric Chemistry and Physics*, Vol. 10, pp. 2745–2764.
- World Health Organization (WHO), 2006, *Air quality guidelines for particulate matter, ozone, nitrogen dioxide and sulfur dioxide - Global update 2005*, Geneva: WHO Press.

APPENDIX A: INTRODUCTION TO ATMOSPHERIC PARTICLES

A.1. PARTICLE SIZES

The size of airborne particles is an important parameter for their dynamic behavior (and impact on human health). In order to gain insight in atmospheric particles, we divide them into different size modes, each with its own characteristic properties.

The nucleation mode consists of particles with a particle diameter D_p between 1 and 10 nm. Particles in this mode are e.g. ion clusters or quantum dots. Small nucleation mode particles can grow through nucleation in a new particle forming event.

The Aitken mode consists of particles $10 < D_p < 100$ nm, also referred to as ultrafine particles. In our atmosphere, particles in this size range have the largest number. Aitken mode particles grow due to coagulation. They are mostly composed of nitrates, sulphates, ammonium, organic compounds and, formed from combustion processes, trace metals (Intech). These particles are able to penetrate deep into the lungs, or be included in the blood stream, and plus, their large surface area may account for extra negative impacts on human health (Tranfield & Walker, 2012).

Accumulation mode consists of particles with aerodynamic diameter between 100-1000 nm. This is the size nanoparticles grow to due to coagulation: nanoparticles that clump together increase in size. After $1\mu\text{m}$ the difference in volume is so large that particles don't grow much due to coagulation with nanoparticles: per coagulation event the volume grows approximately with one millionth.

The coarse particles have diameters between 1 and $10\mu\text{m}$. To this mode belong particles from sea salt sprays, pollen, spores and plant fibres (Intech). They have a typical lifetime of a number of hours; deposition is their main loss effect. When inhaled, they deposit in the upper airways (Intech).

Any particle bigger than $10\mu\text{m}$ is called a giant, or supercoarse particle. These particles, e.g. resuspended road dust, are too big to enter the human respiratory system. They are mostly encountered close to their source, because they quickly settle out of the atmosphere due to their high mass.

A.2. PARTICLE CONCENTRATIONS

Particle sizes are continuous and therefore, number concentrations are not straightforward: in our atmosphere, we do not find 100 particles/cm³ with diameter 100 nm, but 100 particles/cm³ within range 90-110 nm. This is hard to work with: changing width of the range would automatically impact the number concentrations. And, worse: what does the integral over all sizes mean? This is why particles are measured in $dN/d \log D_p$. This way, integrating the curve of number concentrations against radii gives us N , the total number concentration (#/m³).

While particles in the nucleation, Aitken and accumulation modes are measured by number concentration, the coarse and supercoarse modes (particles larger than $1\mu\text{m}$) are measured by their mass concentration. The mass concentration of all suspended particles is expressed as TSP (Total suspended particulate). The mass of all suspended particles with a diameter below $10\mu\text{m}$ is called PM₁₀ (PM stands for particulate matter) and the mass of suspended particles with a diameter below $2.5\mu\text{m}$ is called PM_{2.5}. These categories are mainly introduced as a measure for air pollution and risk to human health.

A.3. PARTICLE SIZE DISTRIBUTIONS

Generally, particle modes can be described as lognormal modes, where a quantity is distributed around a mean diameter μ , with a geometric standard deviation σ_g , which is best explained with an example: a σ_g of 2 means 68% of the measured quantity lies between $\frac{1}{2}\mu$ and 2μ . Note that a σ_g of 1 thus indicates 100% lies at μ itself. Both number and volume concentrations are lognormally distributed; however, volume concentrations grow with N times r^3 whereas number concentrations grow linearly with N . Number densities and mass densities therefore peak at different D_p 's: Number concentration in Aitken mode, mass concentration in coarse mode.

A.4. REFERENCES

Klara Slezakova, Simone Morais and Maria do Carmo Pereira (2013). Atmospheric Nanoparticles and Their Impacts on Public Health, Current Topics in Public Health, Dr. Alfonso Rodriguez-Morales (Ed.), InTech. Available from: <http://www.intechopen.com/books/current-topics-in-public-health/atmospheric-nanoparticles-and-their-impacts-on-public-health> (17-6-2015)

Erin M. Tranfield and David C. Walker (2012). Understanding Human Illness and Death Following Exposure to Particulate Matter Air Pollution, Environmental Health - Emerging Issues and Practice, Prof. Jacques Oosthuizen (Ed.), InTech. Available from: <http://www.intechopen.com/books/environmental-health-emerging-issues-and-practice/understanding-human-illness-and-death-following-exposure-to-particulate-matter-air-pollution> (17-6-2015)

APPENDIX B: TABLES AND FIGURES

D_{p_2} (m) \ D_{p_1} (m)	$1,00 \cdot 10^{-4}$	$3,16 \cdot 10^{-5}$	$1,00 \cdot 10^{-6}$	$3,16 \cdot 10^{-6}$	$1,00 \cdot 10^{-6}$	$3,16 \cdot 10^{-7}$	$1,00 \cdot 10^{-7}$	$3,16 \cdot 10^{-8}$	$1,00 \cdot 10^{-8}$	$3,16 \cdot 10^{-9}$	$1,00 \cdot 10^{-9}$
$1,00 \cdot 10^{-9}$	$1,64 \cdot 10^{-3}$	$5,17 \cdot 10^{-4}$	$1,62 \cdot 10^{-4}$	$5,03 \cdot 10^{-5}$	$1,49 \cdot 10^{-5}$	$3,93 \cdot 10^{-6}$	$7,92 \cdot 10^{-7}$	$1,09 \cdot 10^{-7}$	$1,30 \cdot 10^{-8}$	$1,90 \cdot 10^{-9}$	$6,12 \cdot 10^{-10}$
$3,16 \cdot 10^{-9}$	$1,65 \cdot 10^{-4}$	$5,22 \cdot 10^{-5}$	$1,65 \cdot 10^{-5}$	$5,15 \cdot 10^{-6}$	$1,57 \cdot 10^{-6}$	$4,48 \cdot 10^{-7}$	$1,08 \cdot 10^{-7}$	$1,98 \cdot 10^{-8}$	$3,30 \cdot 10^{-9}$	$1,08 \cdot 10^{-9}$	
$1,00 \cdot 10^{-8}$	$1,70 \cdot 10^{-5}$	$5,39 \cdot 10^{-6}$	$1,70 \cdot 10^{-6}$	$5,37 \cdot 10^{-7}$	$1,67 \cdot 10^{-7}$	$5,08 \cdot 10^{-8}$	$1,46 \cdot 10^{-8}$	$4,08 \cdot 10^{-9}$	$1,76 \cdot 10^{-9}$		
$3,16 \cdot 10^{-8}$	$1,89 \cdot 10^{-6}$	$6,00 \cdot 10^{-7}$	$1,90 \cdot 10^{-7}$	$6,05 \cdot 10^{-8}$	$1,94 \cdot 10^{-8}$	$6,44 \cdot 10^{-9}$	$2,43 \cdot 10^{-9}$	$1,61 \cdot 10^{-9}$			
$1,00 \cdot 10^{-7}$	$2,69 \cdot 10^{-7}$	$8,54 \cdot 10^{-8}$	$2,73 \cdot 10^{-8}$	$8,91 \cdot 10^{-9}$	$3,10 \cdot 10^{-9}$	$1,30 \cdot 10^{-9}$	$9,58 \cdot 10^{-10}$				
$3,16 \cdot 10^{-7}$	$5,80 \cdot 10^{-8}$	$1,86 \cdot 10^{-8}$	$6,10 \cdot 10^{-9}$	$2,16 \cdot 10^{-9}$	$9,51 \cdot 10^{-10}$	$6,96 \cdot 10^{-10}$					
$1,00 \cdot 10^{-6}$	$1,61 \cdot 10^{-8}$	$5,32 \cdot 10^{-9}$	$1,90 \cdot 10^{-9}$	$8,51 \cdot 10^{-10}$	$6,19 \cdot 10^{-10}$						
$3,16 \cdot 10^{-6}$	$5,07 \cdot 10^{-9}$	$1,82 \cdot 10^{-9}$	$8,19 \cdot 10^{-10}$	$5,96 \cdot 10^{-10}$							
$1,00 \cdot 10^{-5}$	$1,79 \cdot 10^{-9}$	$8,10 \cdot 10^{-10}$	$5,89 \cdot 10^{-10}$								
$3,16 \cdot 10^{-5}$	$8,07 \cdot 10^{-10}$	$5,88 \cdot 10^{-10}$									
$1,00 \cdot 10^{-4}$	$5,88 \cdot 10^{-10}$										

Table f.2 Brownian coagulation coefficient K_{12} (cm^3/s) for coagulation of particles diameters D_{p1} and D_{p2} (m). $T=283.15$ K, $\mu=1.77 \cdot 10^{-4}$ g $\text{cm}^{-1}\text{s}^{-1}$. Compare **figure 2**.

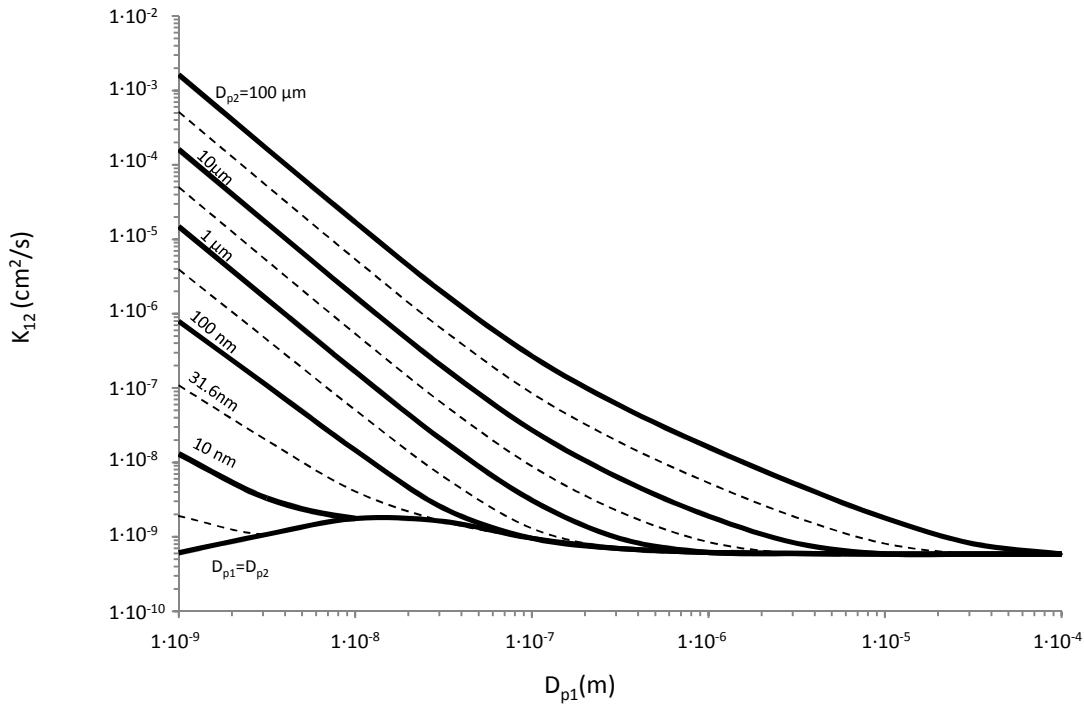


Figure 2 Brownian coagulation coefficient K_{12} (cm^3/s) for coagulation of particles diameters D_{p1} and D_{p2} . Find the smaller of the two particles and then locate the line corresponding to the larger particle. $T=283.15$ K, $\mu=1.77 \cdot 10^{-4}$ g $\text{cm}^{-1}\text{s}^{-1}$.

	Unpaved road ¹³	Urban kerbside ¹⁴	Urban backgr. ^{15,9}	Rural backgr. ¹⁶
TSP _{mean}	1560	122	96/40	24
TSP _{max}	3600	377	466/194	79
TSP _{min}	760	42	15/6	10
PM10 _{mean}	1130	76	23/28	21
PM10 _{max}	2420	214	95/120	53
PM10 _{min}	640	37	1/3	4
PM2.5 _{mean}	570	57	8/19	15
PM2.5 _{max}	1610	122	65/81	48
PM2.5 _{min}	240	28	0.5/2	3

Table 2 Rough indication of mass concentrations in different environments. Concentrations are given in $\mu\text{g}/\text{m}^3$.

	Unpaved road	Urban kerbside ¹⁷	Urban backgr. ¹⁰	Rural backgr. ¹⁸
N _{mean}	unknown	$3 \cdot 10^{10}$	$5 \cdot 10^9$	$4 \cdot 10^9$
N _{max}	unknown	$1 \cdot 10^{11}$	$3 \cdot 10^{10}$	$1 \cdot 10^{10}$
N _{min}	unknown	$6 \cdot 10^9$	$5 \cdot 10^8$	$1 \cdot 10^8$

Table 3 Rough indication of number concentrations in different environments. Concentrations are given in m^{-3} .

	2.37 nm	10 nm	31.6 nm	100nm
1.54 μm	$4.34 \cdot 10^{-6}$	$2.60 \cdot 10^{-7}$	$2.97 \cdot 10^{-8}$	$4.55 \cdot 10^{-9}$
3.16 μm	$9.10 \cdot 10^{-6}$	$5.37 \cdot 10^{-7}$	$6.05 \cdot 10^{-8}$	$8.91 \cdot 10^{-9}$
31.6 μm	$9.26 \cdot 10^{-5}$	$5.39 \cdot 10^{-6}$	$6.00 \cdot 10^{-7}$	$8.54 \cdot 10^{-8}$

Table 4 Coagulation coefficients K_{12} (cm^3/s) for nano-micro coagulation. Compare [figure 5](#).

	2.37 nm	10 nm	31.6 nm	100nm
100 nm	$1.79 \cdot 10^{-7}$	$1.46 \cdot 10^{-8}$	$2.43 \cdot 10^{-9}$	$9.58 \cdot 10^{-10}$
31.6 nm	$3.02 \cdot 10^{-8}$	$4.08 \cdot 10^{-9}$	$1.61 \cdot 10^{-9}$	
10 nm	$4.48 \cdot 10^{-9}$	$1.76 \cdot 10^{-9}$		
2.37 nm	$9.41 \cdot 10^{-10}$			

Table 5 Coagulation coefficients K_{12} (cm^3/s) for nano-nano coagulation. Compare [figure 5](#).

¹³ Chang, 2006

¹⁴ Chan and Kwok, 2001

¹⁵ Bayraktar et al., 2010

¹⁶ Gomisceka, 2004

¹⁷ Wang et al., 2010

¹⁸ Asmi et al., 2011



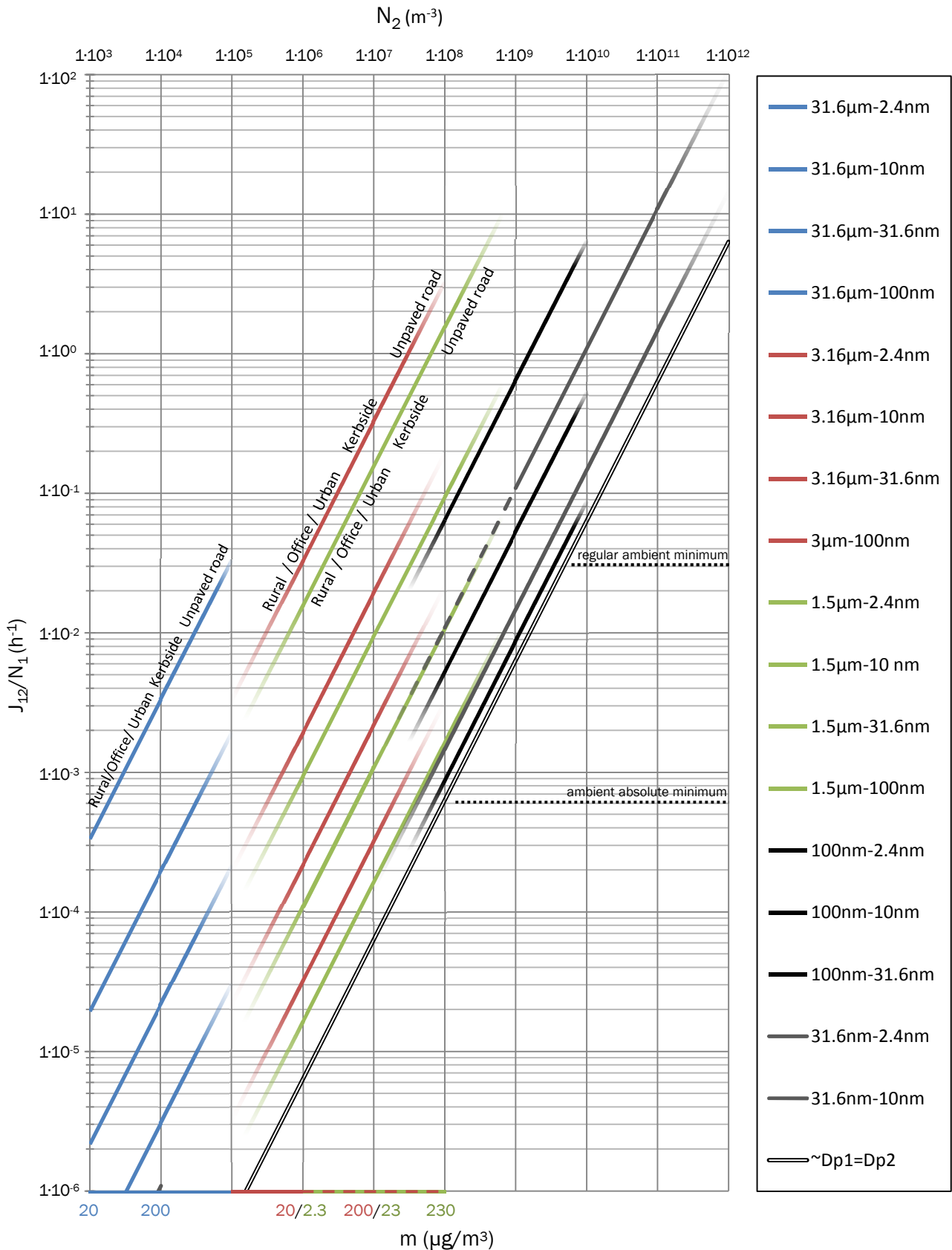


Figure 5 Fractional loss of smaller particles per hour for coagulation of particles diameters D_{p1} and D_{p2} , with growing number of bigger particles $N_2 \text{ (m}^{-3}\text{)}$. Each line represents a combination of a bigger and a smaller particle diameter. Find the line of interest, on the horizontal axis find the total number (upper axis), or the total mass (lower axis) of the bigger particles. Blue indicates particles with (mean) diameter 31.6 µm, a good estimate for TSP; red indicates particles with (mean) diameter 3.16 µm, a good estimate for PM10; green indicated particles with diameter 1.54 µm, a good estimate for PM2.5. One grey line (31 nm-2.4nm) is dashed because of overlap with a green line (1.54 µm-31.6 nm). Lines are labeled at approximate values per environment. Compare [table 2](#). To be correct: N_2 is to be defined as $\int (dN_2/d\text{Log}D_{p,2})d\text{Log}D_p$. $T=283.15 \text{ K}$, $\mu=1.77 \cdot 10^{-4} \text{ g cm}^{-1}\text{s}^{-1}$

		Nanomode			Micromode			Result	
Exp.1		μ	N	σ_g	μ	N	σ_g	Loss (%/h)	Cont/Mono
1.1	1.1.1	10 nm	0.01 cm ⁻³	1	3.16 μ m	10 cm ⁻³	1	1.9	1
	1.1.2						1.5	2.1	1.11
	1.1.3						2	2.5	1.32
1.2	1.2.1	10 nm	0.01 cm ⁻³	1	31.6 μ m	1 cm ⁻³	1	1.6	1
	1.2.2						1.5	2.1	1.31
	1.2.3						2	2.4	1.50
1.3	1.3.1	10 nm	0.01 cm ⁻³	1	1.54 μ m	10 cm ⁻³	1	0.93	1
	1.3.2						1.5	1.01	1.09
	1.3.3						2	1.19	1.28
Exp.2		μ	N	σ_g	μ	N	σ_g	Loss (%/h)	Cont/Mono
2.1	2.1.1	2.37 nm	0.01 cm ⁻³	1	3.16 μ m	1 cm ⁻³	1	3.2	1
	2.1.2			1.5				4.1	1.28
	2.1.3			2				4.5	1.41
2.2	2.2.1	10 nm	0.01 cm ⁻³	1	3.16 μ m	10 cm ⁻³	1	1.9	1
	2.2.2			1.5				2.9	1.53
	2.2.3			2				4.9	2.58
2.3	2.3.1	31.6 nm	0.01 cm ⁻³	1	3.16 μ m	10 cm ⁻³	1	0.22	1
	2.3.2			1.5				0.34	1.55
	2.3.3			2				0.62	2.82
2.4	2.4.1	100 nm	0.01 cm ⁻³	1	3.16 μ m	10 cm ⁻³	1	0.031	1
	2.4.2			1.5				0.041	1.32
	2.4.3			2				0.065	2.10
Exp.3		μ	N	σ_g	μ	N	σ_g	Loss (%/h)	Cont/Mono
3.1	3.1.1	2.37 nm	0.01 cm ⁻³	1	3.16 μ m	1 cm ⁻³	1	3.2	1
	3.1.2			1.5			5.5	1.72	
	3.1.3			2			5.9	1.84	
3.1	3.2.1	10 nm	0.01 cm ⁻³	1	3.16 μ m	10 cm ⁻³	1	1.9	1
	3.2.2			1.5			3.4	1.80	
	3.2.3			2			5.0	2.63	
3.3	3.3.1	31.6 nm	0.01 cm ⁻³	1	3.16 μ m	10 cm ⁻³	1	0.22	1
	3.3.2			1.5			0.38	1.73	
	3.3.3			2			0.69	3.14	

Table 6 Coagulation loss of particles in the nanomode after 1 hour. The column 'Cont/mono' indicates the fraction of continuously calculated loss over monodispersely calculated loss. Input as described for experiments 1,2 and 3 in the method section. A σ_g of 1 indicates a monodisperse result; however, The UHMA-model does not allow a σ_g of 1. Monodisperse coagulation losses are either obtained through multiplication of K_{12} with N_2 (method used in figure 5), or through a model run with a σ_g of 1.0001: a value small enough to ensure all particles will be placed in the same size bin. These methods lead to the same results.